Essential role for $G\alpha_{13}$ in endothelial cells during embryonic development

Kathleen M. Ruppel*†‡, David Willison*‡, Hiroshi Kataoka*, Alice Wang*, Yao-Wu Zheng*, Ivo Cornelissen*, Liya Yin*, Shan Mei Xu*, and Shaun R. Coughlin*§¶‖

*Cardiovascular Research Institute and Departments of †Pediatrics, §Medicine, and ¶Cellular and Molecular Pharmacology, University of California, San Francisco, CA 94143

Contributed by Shaun R. Coughlin, April 23, 2005

Toward identifying the roles of protease-activated receptor-1 (PAR1) and other G protein-coupled receptors important for vascular development, we investigated the role of $G\alpha_{13}$ in endothelial cells in the mouse embryo. LacZ inserted into *$G\alpha_{13}$* exon 1 was highly expressed in endothelial cells at midgestation. Endothelial-specific *$G\alpha_{13}$* knockout embryos died at embryonic days 9.5–11.5 and resembled the PAR1 knockout. Restoration of $G\alpha_{13}$ expression in endothelial cells by use of a Tie2 promoter-driven $G\alpha_{13}$ transgene rescued development of endothelial-specific *$G\alpha_{13}$* knockout embryos as well the embryonic day 9.5 vascular phenotype in *$G\alpha_{13}$* conventional knockouts; transgene-positive *$G\alpha_{13}^{-/-}$* embryos developed for several days beyond their transgene-negative *$G\alpha_{13}^{-/-}$* littermates and then manifested a previously uncharacterized phenotype that included intracranial bleeding and exencephaly. Taken together, our results suggest a critical role for $G\alpha_{13}$ in endothelial cells during vascular development, place $G\alpha_{13}$ as a candidate mediator of PAR1 signaling in this process, and reveal roles for $G\alpha_{13}$ in other cell types in the mammalian embryo.

angiogenesis | endothelial cell | G protein | G protein-coupled receptor | G13

Formation of blood vessels during mammalian embryonic development is a complex and highly regulated process. Angioblasts proliferate, migrate, and differentiate to form primitive vascular structures composed of endothelial cells. These structures remodel by sprouting, branching, growing, and regressing, and mature by the recruitment and differentiation of pericytes and smooth muscle cells (1–3). Studies to define the molecular signals that orchestrate vascular development have focused mainly on receptor tyrosine kinases and integrins and their ligands (1, 4–9). Less is known regarding the roles of G protein-coupled receptors (GPCRs) in this process (10–16).

Protease-activated receptor-1 (PAR1), a GPCR for thrombin, plays an important role in the formation and/or maintenance of blood vessels in mouse embryos, a role likely attributable to PAR1 function in endothelial cells (11, 14). PAR1 triggers a host of cellular responses through heterotrimeric G proteins of the Gq/11, Gi/o, and G12/13 families; which of these pathways is important for proper vascular development is unknown. Conventional knockout of the gene-encoding $G\alpha_{13}$ caused death of mouse embryos at midgestation with a phenotype grossly similar to, but more penetrant than, the PAR1 phenotype (17). We report a key role for $G\alpha_{13}$ in endothelial cells at midgestation, suggesting that loss of $G\alpha_{13}$ signaling in endothelial cells may account for the embryonic phenotype associated with PAR1 deficiency. Our results also unmask roles for $G\alpha_{13}$ in other cell types.

Materials and Methods

Mutant Mouse Strains. ***Generation of the $G\alpha_{13}$-lacZ knockin allele.*** *Gna13* (herein designated $G\alpha_{13}$) gene fragments from a bacterial artificial chromosome from a 129/SvJ mouse genomic library, along with the *lacZ* gene, were used to construct a $G\alpha_{13}$-lacZ knockin allele as described in *Supporting Methods*, which is published as supporting information on the PNAS web site, and Fig. 1. The loxP-flanked *neo*^{r} cassette was excised *in vivo* by crossing mice heterozygous for the $G\alpha_{13}$-lacZ-Neo allele to mice carrying a β-actin promoter-Cre transgene (18).

Generation of a floxed $G\alpha_{13}$ allele. $G\alpha_{13}$ gene fragments from BAC-125h06 were used to construct a conditional allele for Cre-*lox* mediated excision of $G\alpha_{13}$ as described in *Supporting Methods* and Fig. 2. Cre-mediated excision of the flox allele generated a null $G\alpha_{13}$ allele ("Δ4"), transcription of which gives rise to an mRNA fragment encoding a truncated $G\alpha_{13}$ protein predicted to be inactive and short-lived.

Generation of Tie2-$G\alpha_{13}$ transgenic mice. A transgene to direct $G\alpha_{13}$ expression to endothelium was generated by inserting $G\alpha_{13}$ coding sequence along with an internal ribosome entry sequence (19), into pBS-Tie2-*lacZ* (from Thomas Sato, University of Texas Southwestern, Dallas) as described in *Supporting Methods* and Fig. 5. Two independent transgenic lines that showed endothelial-specific β-gal staining in embryonic day (E)8.5–11.5 embryos were selected for study. Similar results were obtained with each of the two lines.

Other Mouse Strains. *Tie2-Cre* and *Tie2-lacZ* were from T. Sato and M. Yanagisawa, respectively (University of Texas Southwestern) (20, 21), and *β-actin-Cre* and *-FLP* from J. Miyazaki (Osaka University Medical School, Osaka) (18) and S. M. Dymecki (Carnegie Institute of Washington, Baltimore) (22), respectively. The *ROSA26R* Cre reporter strain (23) was from The Jackson Laboratory. $G\alpha_{13}^{+/-}$ (exon 1 deletion) mice were from M. Simon (California Institute of Technology, Pasadena, CA) (17).

Genotyping of Mutant Mouse Strains. DNA was isolated from ES cell clones, embryos, or mouse tail samples (14) and genotyped for $G\alpha_{13}$ wild-type (WT), flox, Δ4, and (−) alleles by digestion with EcoRV and NcoI and Southern hybridization with "exon 1" and "exon 4" probes (Fig. 2). $G\alpha_{13}$-*lacZ* and $G\alpha_{13}$-*lacZ-Neo* alleles were genotyped by NcoI digestion and Southern hybridization with the exon 1 probe (Fig. 1). The *Tie2-*$G\alpha_{13}$ and *Tie2-lacZ* transgenes were detected by Southern blot analysis with a *lacZ* cDNA probe. The *Tie2-Cre* and *β-actin-Cre* transgenes were detected either by PCR or Southern blot for *Cre* sequence. Southern and Northern analyses were performed by using standard techniques.

Embryo Dissection, Immunostaining, and X-Gal Staining. Noon of the day a vaginal plug was observed was defined as E0.5. After killing, the uterine horns were removed and embryonic and extraembryonic tissues were dissected free. After photographing the yolk sac and noting its properties, the yolk sac was opened, and the embryo was examined for gross phenotypes, then X-Gal was stained or immunostained in whole mount (24) or sections as described in *Supporting Methods*.

Abbreviations: E*n*, embryonic day *n*; GPCR, G protein-coupled receptor; PAR1, protease-activated receptor-1.

‡K.M.R. and D.W. contributed equally to this work.

‖To whom correspondence should be addressed. E-mail: coughlin@cvrimail.ucsf.edu.

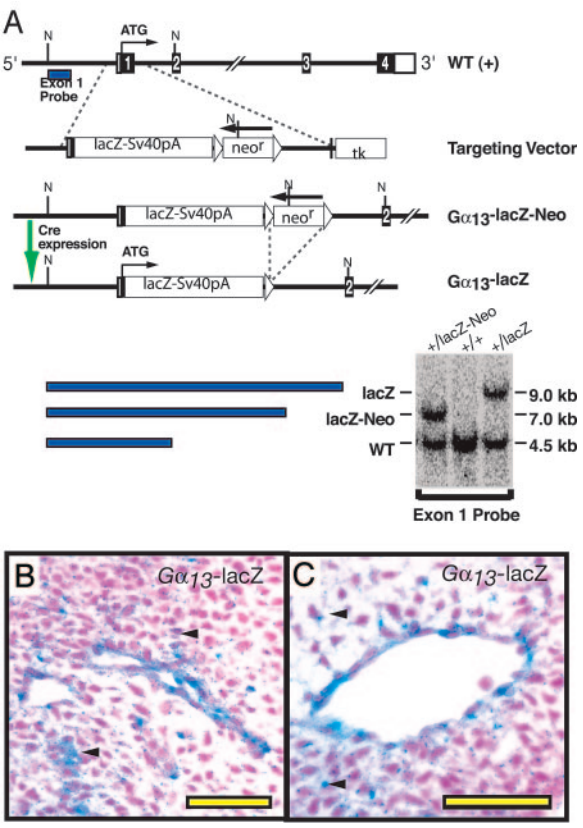

Fig. 1. *Gα13-lacZ* knockin allele. (*A*) Diagram of the WT *Gα13* locus, the *Gα13-lacZ* targeting vector, and the recombined locus. Exons (coding in black, untranslated in open boxes), loxP sites (△), and neomycin resistance (*neo^r*) and thymidine kinase negative selection (*tk*) cassettes are shown. The expected sizes of DNA fragments detected by Southern blot analysis by using ''Exon 1'' probe after an NcoI digest along with Southern blot of tail DNA from mice with the indicated *Gα13* alleles are at bottom. (*B* and *C*) Analysis of tissue sections from an E10.5 $G\alpha_{13}^{+/lacZ}$ revealed some staining throughout the mesenchyme (arrows) and stronger staining in the endothelium; intersomitic (*B*) and head (*C*) vessels are shown.

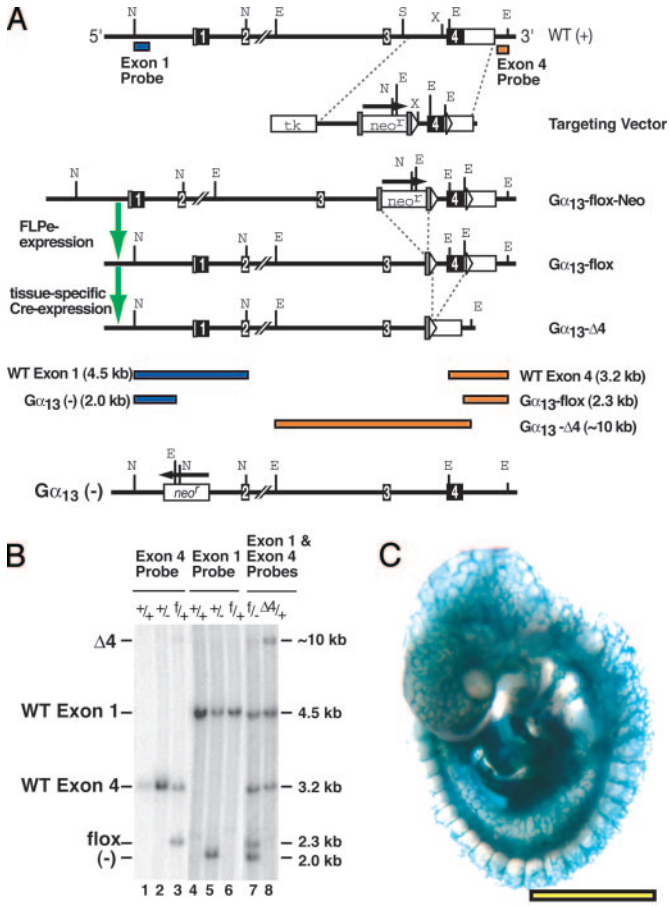

Fig. 2. Floxed *Gα13* allele. (*A*) Diagram of WT *Gα13* locus, targeting vector, recombined locus along with FLPe-excised ''flox'' allele, and Cre-excised ''Δ4'' null allele. Shaded rectangles indicate FRT sites; other conventions are as in Fig. 1. Shown at *Bottom* is the constitutive null *Gα13* allele (''−'') described in ref. 17. Sizes of the DNA fragments detected by Southern hybridization with either Exon 1 (blue) or Exon 4 (orange) probe after NcoI/EcoRV digestion are shown in *Bottom*. (*B*) Southern blot analysis of tail DNA from adult mice with the indicated *Gα13* genotypes: WT (+), exon 1 constitutive null (−), flox (f), exon 4 deletion null (Δ4). The probes used are indicated at the top. The DNA in lane 8 was obtained from a *β-actin-Cre* transgene-positive mouse; note the absence of the 2.3 kb *Gα13* flox allele band and the presence of the ≈10.0 kb *Gα13* Δ4 allele band. (*C*) Efficient endothelium-specific excision by *Tie2-Cre*. *Tie2-Cre*$^{Tg/o}$;*ROSA26R* embryos collected at E9.5 were X-Gal stained. Virtually all endothelial cells were lacZ positive. (Scale bar: 1 mm.)

Isolation and Adenoviral Infection of Neonatal Endothelial Cells. Microvascular endothelial cells were isolated from the skin of $G\alpha_{13}^{flox/flox}$ neonates. More than 95% of cells in these preparations expressed the endothelial markers PECAM1 and ICAM2 (25). Immediately after the second round of immunopurification, cells were subjected to two successive infections with ≈100 infections units/ml of Cre-GFP or GFP only adenovirus (from Hilary Beggs, University of California, San Francisco) for 24 h each (26, 27); titers were determined by using an adenoviral titer kit (Clontech). One to 6 days after the second infection, the cells were used for experiments. $G\alpha_{13}$ mRNA expression was nearly ablated in $G\alpha_{13}^{flox/flox}$ endothelial cells infected with the Cre adenovirus (data not shown).

Matrigel Assay. Endothelial cells (1×10^5) that had been infected with the appropriate adenovirus were plated onto a Matrigel surface and incubated 14–16 h at 37°C in DMEM with 20% FBS and 50 μg/ml endothelial cell growth supplement (BTI, Stoughton, MA) as described in *Supporting Methods*. PHOTOSHOP 7.0 (Adobe Systems, San Jose, CA) was used to perform planimetry to determine area covered by cells.

Results

To characterize *Gα13* expression in the mouse embryo, we generated a mouse bearing a *Gα13* lacZ knockin allele (*Gα13* lacZ allele; Fig. 1) such that lacZ transcription would mimic that of *Gα13*. X-Gal staining of E10.5 $G\alpha_{13}^{+/lacZ}$ embryos revealed lacZ activity throughout the mesenchyme and stronger staining in vascular endothelial cells and dorsal neural tube (Fig. 1 and data not shown). *Gα13* expression was also readily detected by Northern analysis of endothelial cells immunopurified from neonatal mice (25) and by X-Gal staining of endothelial cells from $G\alpha_{13}^{+/lacZ}$ mice (data not shown). In the context of the phenotype of the conventional *Gα13* knockout (17), these results prompted an effort to define the importance $G\alpha_{13}$ function in endothelial cells.

We generated mice bearing a *Gα13* conditional allele in which the coding portion of exon 4 was flanked by loxP sites (Fig. 2). Mice with one such "floxed" and one WT allele ($G\alpha_{13}^{+/flox}$) were mated to each other and to mice heterozygous for the conventional exon 1 knockout *Gα13* allele ($G\alpha_{13}^{+/-}$) (17) to generate $G\alpha_{13}^{flox/flox}$ and $G\alpha_{13}^{flox/-}$ offspring. These offspring were born at or near the expected Mendelian rate and had no obvious abnormalities. Thus, insertion of loxP sites did not disrupt necessary functions of the *Gα13* gene.

Table 1. Impaired viability of endothelial-specific $G\alpha_{13}$ knockout mice

Breed	+/flox	+/−	−/−	flox/−
Tie2-Cre$^{Tg/o}$	38	29	0	3
Tie2-Cre$^{o/o}$	40	33	0	25

DNA was collected from 168 offspring from a *Tie2-Cre*$^{Tg/o}$, $G\alpha_{13}^{+/-}$ × $G\alpha_{13}^{flox/-}$ intercross alive at ≈postnatal day 10.

$G\alpha_{13}^{flox/flox}$ mice were mated to mice carrying a β-actin promoter-driven Cre transgene (18) to generate offspring heterozygous for the $G\alpha_{13}$ exon 4 deletion ($G\alpha_{13}^{+/\Delta4}$). Southern blot (Fig. 2) and PCR analysis (data not shown) confirmed excision of exon 4. $G\alpha_{13}^{+/\Delta4}$ mice were intercrossed to generate $G\alpha_{13}^{\Delta4/\Delta4}$ embryos, which died at ≈E9.5 with a phenotype indistinguishable from that reported for embryos homozygous for a $G\alpha_{13}$ exon 1 deletion allele ($G\alpha_{13}^{-/-}$) (17); $G\alpha_{13}^{\Delta4/-}$ embryos also exhibited the $G\alpha_{13}^{-/-}$ phenotype (data not shown). Thus, Cre-mediated excision of $G\alpha_{13}$ exon 4 resulted in a $G\alpha_{13}$ allele that was functionally null.

We used a *Tie2-Cre* transgene (20, 21) to excise the $G\alpha_{13}$ flox allele expression in endothelium. Such ablation of $G\alpha_{13}$ function in endothelial cells resulted in a highly penetrant embryonic lethal phenotype. $G\alpha_{13}^{flox/-}$ mice were crossed with $G\alpha_{13}^{+/-}$ mice hemizygous for the *Tie2-Cre* transgene (*Tie2-Cre*$^{Tg/o}$; $G\alpha_{13}^{+/-}$), and offspring were genotyped ≈10 days after birth (Table 1). Live $G\alpha_{13}^{flox/+}$ or $G\alpha_{13}^{+/-}$ offspring were produced at similar rates in the presence or absence of the transgene. By contrast, *Tie2-Cre*$^{Tg/o}$; $G\alpha_{13}^{flox/-}$ mice, hereafter referred to as $G\alpha_{13}$ endoKO, were markedly underrepresented compared with their Cre-negative counterparts (3 vs. 25; $P < 0.005$). The few $G\alpha_{13}$ endoKO mice that were born were runted.

The $G\alpha_{13}$ endoKO embryonic phenotype was highly penetrant by midgestation (Table 2). Embryos from *Tie2-Cre*$^{Tg/Tg}$; $G\alpha_{13}^{+/-}$ × $G\alpha_{13}^{flox/-}$ matings were collected at E8.5, 9.5, 10.5, and 11.5. At E8.5, the resulting $G\alpha_{13}^{-/-}$ and $G\alpha_{13}$ endoKO embryos were indistinguishable from their $G\alpha_{13}^{+/-}$ and $G\alpha_{13}^{+/flox}$ littermates in gross appearance. At E9.5, about one-half of $G\alpha_{13}^{-/-}$ embryos were dead and all were abnormal. $G\alpha_{13}$ endoKO embryos were also severely affected at this time; 36% were dead and 76% were affected (Table 2). By E10.5, ≈90% of $G\alpha_{13}^{-/-}$ and 50% of $G\alpha_{13}$ endoKO embryos were dead; all $G\alpha_{13}^{-/-}$ embryos and 81% of $G\alpha_{13}$ endoKO embryos were affected. By E11.5, all $G\alpha_{13}^{-/-}$ and 88% of $G\alpha_{13}$ endoKO embryos were dead.

The gross features of the $G\alpha_{13}$ endoKO phenotype were similar to, but somewhat less severe than, those of the conventional $G\alpha_{13}$ knockout (17). Both had wrinkled yolk sacs with a paucity of blood-filled vessels as well as pale and delayed embryos with pericardial swelling and variable bleeding into cavities and tissues (Figs. 3 and 4). The onset and penetrance of developmental delay and pericardial dilatation was similar in $G\alpha_{13}^{-/-}$ embryos and $G\alpha_{13}$ endoKO embryos, but gross hemorrhage was more evident in the former.

Table 2. Genotype and gross phenotype of embryos from *Tie2-Cre*$^{+/+}$; $G\alpha_{13}^{+/-}$ × $G\alpha_{13}^{flox/-}$ intercrosses

	$G\alpha_{13}$ genotype, alive/total (% abnormal)			
Age	flox/+	+/−	−/−	flox/−
E9.5	27/32 (13)	29/34 (9)	11/21 (100)	16/25 (76)
E10.5	21/23 (9)	20/22 (9)	2/19 (100)	8/16 (81)
E11.5	17/20 (15)	27/29 (10)	0/13 (100)	3/24 (92)

Alive/total number of embryos recovered and the percent of abnormal embryos for each genotype at the indicated gestational age are shown. Alive was defined as having a heartbeat. Abnormal included embryos showing pericardial dilatation, hemorrhage, developmental delay, or absence of a heartbeat. Note that all embryos generated by this cross were *Tie2-Cre*$^{Tg/o}$.

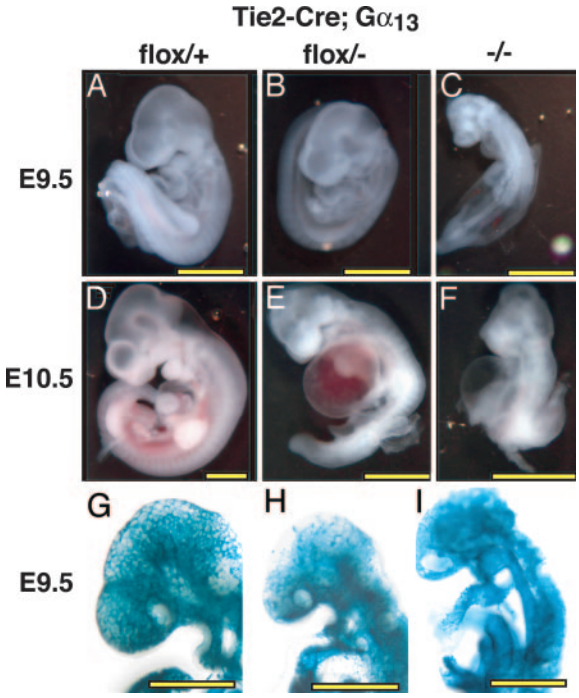

Fig. 3. Phenotype of $G\alpha_{13}$ endothelial-specific knockout and $G\alpha_{13}^{-/-}$ embryos. All embryos are *Tie2-Cre*$^{Tg/o}$ and had a heartbeat at the time of photography. (*A–F*) Gross appearance of $G\alpha_{13}^{+/+}$ embryos (*A* and *D*), $G\alpha_{13}^{flox/-}$ embryos (*B* and *E*), and $G\alpha_{13}^{-/-}$ embryos (*C* and *F*). At E9.5 (*A–C*), $G\alpha_{13}^{-/-}$ embryos (*C*) were significantly delayed compared with control embryos (*A*); developmental arrest appeared to occur at ≈E8.5 as reported in ref. 17. $G\alpha_{13}$ endoKO embryos (*B*) had turned and appeared arrested at ≈E9.0. By E10.5 (*D–F*), >80% of $G\alpha_{13}$ endoKO embryos (*E*) were either dead or morphologically abnormal, and all $G\alpha_{13}^{-/-}$ embryos (*F*) were dead or grossly abnormal. Dilated pericardial sacs, consistent with cardiovascular failure, were a prominent feature in both. (*G–I*) Whole-mount X-Gal staining of *Tie2-Cre*$^{Tg/o}$; ROSA26R embryos that were $G\alpha_{13}^{+/+}$ (*G*), $G\alpha_{13}^{flox/-}$ (*H*), and $G\alpha_{13}^{-/-}$ (*I*); embryos were collected at E9.5. Note that there is more primitive vascular plexus in the head of $G\alpha_{13}$ endoKO (*H*) and global $G\alpha_{13}$ nulls (*I*) compared with the control (*G*). (Scale bars: 1 mm.)

The structure of the yolk sacs of $G\alpha_{13}$ endoKO embryos was strikingly abnormal. At E9.5 and E10.5, WT yolk sacs contain an arborized vasculature with large and small vessels evident by gross examination and by PECAM staining. By contrast, large vessels were lacking from $G\alpha_{13}$ endoKO yolk sacs, and unusually large vascular spaces were apparent on cross section (Fig. 4). This finding was even more obvious in $G\alpha_{13}^{-/-}$ yolk sacs.

Whole-mount X-Gal staining of E9.5 $G\alpha_{13}$ endoKO embryos that carried the ROSA26R excision reporter revealed a grossly normal vascular pattern in the trunk (see intersomitic vessels, branchial arch vessels, and endocardium in Fig. 3). However, head vessels showed delayed development and were disorganized compared with those seen in littermate controls (Fig. 3). Similar results were seen by immunostaining for the endothelial markers PECAM and endoglin (data not shown). Thus, endothelial cell differentiation and early vasculogenesis and patterning were relatively normal in embryos that lacked $G\alpha_{13}$ function in endothelial cells, but subsequent remodeling of the vasculature was markedly impaired in several vascular beds.

The results described above strongly suggest that $G\alpha_{13}$ expression in endothelial cells is required for normal vascular development in mouse embryos, but the greater severity of the $G\alpha_{13}^{-/-}$ vs. $G\alpha_{13}$ endoKO phenotype might reflect a necessary role for $G\alpha_{13}$ in other cell types. To probe this question, we asked whether $G\alpha_{13}$ expres-

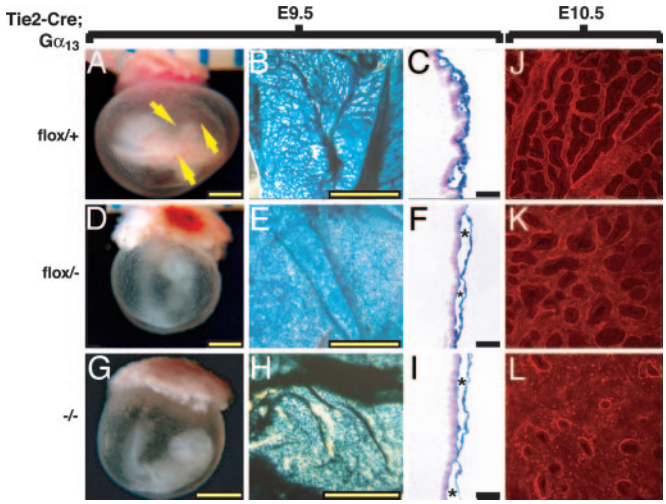

Fig. 4. Phenotype of $G\alpha_{13}$ endoKO and $G\alpha_{13}{}^{-/-}$ yolk sacs. $G\alpha_{13}$ genotypes were flox/+ (*A–D*), flox/− (*E–H*), and −/− (*I–L*). At E9.5, large blood-filled vessels (arrows) were seen in control (*A*) but not in flox/− (*E*) or −/− (*I*) yolk sacs, which were pale and dimpled. X-Gal staining of *Tie2-Cre*$^{Tg/o}$; *ROSA26R* (*B*, *C*, *F*, and *G*) or *Tie2-lacZ*$^{Tg/o}$ (*J* and *K*) yolk sacs revealed an arborized structure with large and small vessels $G\alpha_{13}$ WT (*B*), whereas $G\alpha_{13}$ endoKO (*F*) and $G\alpha_{13}{}^{-/-}$ (*J*) yolk sacs exhibited a more plexus-like structure that lacked large vessels. Cross sections of such yolk sacs (*C*, *G*, and *K*) showed blood-filled vessels spaced at regular intervals and lined with blue-stained endothelial cells in controls (*C*) but enlarged and often bloodless vascular spaces (*) in $G\alpha_{13}$ endoKO (*F*) and $G\alpha_{13}{}^{-/-}$ (*I*) yolk sacs. (Yellow bars: 1 mm; black bars: 100 μm.) (*D*, *H*, and *L*) Immunofluorescence staining of E10.5 yolk sacs for the endothelial marker PECAM1: $G\alpha_{13}{}^{flox/+}$ (*D*), $G\alpha_{13}$ endoKO (*H*), and $G\alpha_{13}{}^{-/-}$ (*L*).

sion in endothelial cells might be sufficient to rescue development of $G\alpha_{13}{}^{-/-}$ embryos. We used the Tie2 promoter/enhancer (20) to drive transcription of a Gα13-IRES-lacZ cassette in endothelial cells in transgenic mice (Fig. 5). X-Gal staining of embryos from two such *Tie2-*$G\alpha_{13}$ transgenic lines confirmed transgene expression in vascular structures from E8.5 onward. Staining was restricted to endothelium and endocardium and to a small fraction of hematopoietic cells, suggesting that transgene expression was appropriately cell-type specific (Fig. 5 and data not shown).

$G\alpha_{13}{}^{+/-}$ mice hemizygous for the endothelial-specific Gα13 transgene (*Tie2-*$G\alpha_{13}{}^{Tg/o}$; $G\alpha_{13}{}^{+/-}$) were crossed to $G\alpha_{13}{}^{+/-}$ mice and embryos collected at various times. Although approximately half of the transgene-negative $G\alpha_{13}{}^{-/-}$ embryos recovered at E9.5 were dead and the remainder were delayed and/or otherwise abnormal, transgene-positive $G\alpha_{13}{}^{-/-}$ embryos were recovered at the expected Mendelian rate, alive and indistinguishable from their $G\alpha_{13}{}^{+/+}$ and $G\alpha_{13}{}^{+/-}$ littermates (Table 3 and Fig. 5). Moreover, whereas transgene-negative $G\alpha_{13}{}^{-/-}$ yolk sacs showed a grossly abnormal vascular plexus (Fig. 4), transgene-positive $G\alpha_{13}{}^{-/-}$ yolk sacs displayed a pattern of branching vessels indistinguishable from that seen in WT littermates (Fig. 5). Thus, expression of Gα13 in endothelial cells was sufficient to prevent vascular defects and death of $G\alpha_{13}{}^{-/-}$ embryos at E9.5.

$G\alpha_{13}{}^{-/-}$ embryos carrying the *Tie2-*$G\alpha_{13}$ transgene survived for several days beyond their transgene-negative counterparts and then developed a second phenotype characterized by exencephaly and hemorrhage within the head mesenchyme (K. Ruppel and S. Coughlin, unpublished data). To determine whether the inability of the *Tie2-*$G\alpha_{13}$ transgene to completely rescue development of $G\alpha_{13}{}^{-/-}$ embryos was due to a requirement for Gα13 function in another cell type vs. failure of the transgene to adequately reproduce the normal level or temporal and spatial pattern of Gα13 expression in endothelial cells, we asked whether the *Tie2-*$G\alpha_{13}$ transgene would completely rescue the endothelial-specific $G\alpha_{13}$ knockout. *Tie2-*$G\alpha_{13}{}^{Tg/o}$; $G\alpha_{13}{}^{flox/-}$

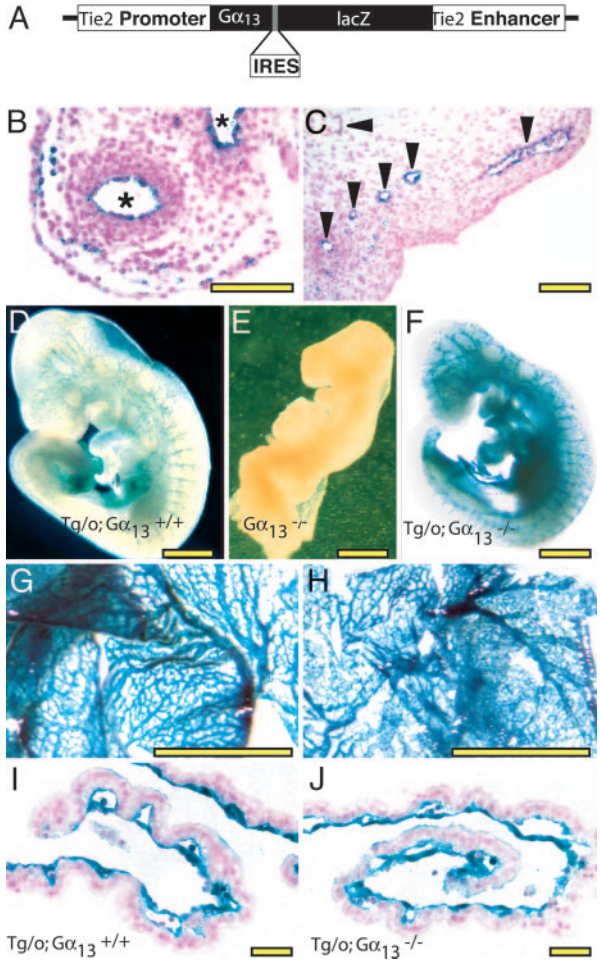

Fig. 5. An endothelium-specific $G\alpha_{13}$ transgene rescues early lethality in $G\alpha_{13}{}^{-/-}$ embryos. (*A*) Tie2 promoter/enhancer-$G\alpha_{13}$-IRES-*lacZ* construct (*Tie2-*$G\alpha_{13}$) used to generate mice in which $G\alpha_{13}$ is expressed in endothelial cells. (*B* and *C*) X-Gal staining of E10.5 embryo showing expression of *Tie2-*$G\alpha_{13}$ in endothelial and occasional hematopoietic cells in umbilical artery and vein (*B*, *) and head vessels (*C*, arrowheads). (*D–F*). Whole-mount X-Gal staining of E9.5 embryos. *Tie2-*$G\alpha_{13}$-positive $G\alpha_{13}{}^{-/-}$ (*F*) embryos were indistinguishable from $G\alpha_{13}{}^{+/+}$ (*D*) embryos and showed normal vascular staining. $G\alpha_{13}{}^{-/-}$ embryos that lacked the transgene (*E*) were all grossly abnormal at this time. (Scale bar = 1 mm.) Whole-mount (*G* and *H*) and cross section (*I* and *J*) of X-Gal stained E9.5 yolk sacs. *Tie2-*$G\alpha_{13}{}^{Tg/o}$; $G\alpha_{13}{}^{+/-}$ mice were mated to $G\alpha_{13}{}^{+/-}$ mice that were homozygous for the Tie2-*lacZ* transgene to generate embryos with strong lacZ expression in endothelial cells. The yolk sac vasculature from both $G\alpha_{13}{}^{+/+}$ (*G* and *I*) and $G\alpha_{13}{}^{-/-}$ (*H* and *J*) embryos that carried the *Tie2-*$G\alpha_{13}$ transgene appeared normal. Note the striking contrast with $G\alpha_{13}{}^{-/-}$ yolk sacs that lacked the transgene (Fig. 4 *H* and *I*). (Scale bars: *B* and *C*, 50 μm; *D–H*, 1 mm; *I* and *J*, 100 μm.)

mice were crossed to $G\alpha_{13}{}^{+/-}$ mice homozygous for the *Tie2-Cre* transgene (*Tie2-*$Cre^{Tg/Tg}$; $G\alpha_{13}{}^{+/-}$). Offspring were genotyped 10–15 days after birth (Table 4). No $G\alpha_{13}{}^{-/-}$ mice were recovered, even when the endothelial-specific $G\alpha_{13}$ transgene was present, and no *Tie2-*$Cre^{Tg/o}$; $G\alpha_{13}{}^{flox/-}$ pups were recovered in the absence of the transgene. By contrast, *Tie2-*$G\alpha_{13}{}^{Tg/o}$; *Tie2-*$Cre^{Tg/o}$; $G\alpha_{13}{}^{flox/-}$ mice were recovered at the expected Mendelian rate. These results suggest that the *Tie2-*$G\alpha_{13}$ transgene drives Gα13 expression in a manner adequate to support the Gα13 functions in endothelial cells that are necessary for embryonic development. Thus, the contrast between the phenotypes of endothelial-specific Gα13 knockout vs. conventional Gα13 knockouts carrying the *Tie2-*$G\alpha_{13}$ transgene is likely due to a necessary role for Gα13 in a cell type(s) other than endothelial

Table 3. Endothelial $G\alpha_{13}$ transgene rescue of $G\alpha_{13}$ early lethality: Genotype and gross phenotype of embryos from *Tie2-*$G\alpha_{13}^{Tg/o}$; $G\alpha_{13}^{+/-} \times G\alpha_{13}^{+/-}$ intercrosses

		Alive/total embryos (% abnormal)					
		$G\alpha_{13}^{+/+}$		$G\alpha_{13}^{+/-}$		$G\alpha_{13}^{-/-}$	
Age	Total	Tg/o	o/o	Tg/o	o/o	Tg/o	o/o
E9.5	90	11/11 (0)	9/9 (0)	23/23 (0)	23/23 (0)	11/11 (0)	6/13 (100)
E11.5	104	15/15 (0)	12/12 (0)	28/28 (0)	25/25 (0)	13/14 (100)	0/10 (100)
E12.5	151	21/22 (5)	16/16 (0)	49/49 (0)	44/46 (4)	2/18 (100)	0/0 (NA)

Number of alive/total recovered embryos and percent of embryos that were abnormal. ''Abnormal'' includes embryos showing hemorrhage, pericardial dilatation, small size, developmental delay, and/or a neural tube defect in addition to those lacking a heart beat. Note that the transgene yielded complete rescue of $G\alpha_{13}^{-/-}$ embryos through E9.5 and nearly complete rescue at the level of viability through E11.5, at which time the rescued embryos manifested a new phenotype (see text). NA, not applicable.

cells, a role that becomes apparent only when $G\alpha_{13}^{-/-}$ embryos are supported beyond E9.5 by the endothelial transgene.

Our results strongly suggest that $G\alpha_{13}$ signaling in endothelial cells plays a critical role in vascular development. What function(s) might it serve in this context? $G\alpha_{13}$ links GPCRs to Rho activation and, perhaps, to other effector pathways. Toward exploring the effect of $G\alpha_{13}$ deficiency on endothelial cell responses and behaviors, we ablated $G\alpha_{13}$ function in cultured mouse microvascular endothelial cells. Cells were immunopurified from the skin of $G\alpha_{13}^{flox/flox}$ neonatal mice and infected with adenovirus-directing expression of Cre and GFP or GFP alone (27). Southern and Northern blot analysis of such cultures suggested an efficiency of >95% for $G\alpha_{13}$ excision (data not shown). Curiously, $G\alpha_{13}$ excision had no detectable effect on Rho activation, changes in endothelial cell shape or stress fiber formation in response to PAR1 agonist, and no effect was detected in assays of endothelial cell movement on coverslips, adhesion on various matrices, or contraction of collagen gels (data not shown). There was, however, a reproducible difference in the behavior of cells cultured on Matrigel. WT or Ad-GFP $G\alpha_{13}^{flox/flox}$ endothelial cells plated on Matrigel formed a monolayer that remodeled to become a "network" of cords and tubes (Fig. 6). Ad-Cre-GFP $G\alpha_{13}^{flox/flox}$ endothelial cells plated at the same density formed a monolayer normally, but subsequent remodeling was markedly decreased (Fig. 6). The different remodeling behaviors depended on the $G\alpha_{13}$ genotype in that no differences were seen in WT cells infected with the Ad-Cre-GFP vs. Ad-GFP viruses. Thus, $G\alpha_{13}$ may be necessary for regulating cell shape, movement, and/or interaction with extracellular matrix during remodeling of endothelial structures.

Discussion

The roles of the >300 nonodorant GPCRs in mammals in embryonic development are relatively unexplored; the number of these receptors and partially redundant functions of some family members makes a systematic study of the necessary roles of GPCRs in development a daunting proposition. Probing for roles of GPCRs by ablation of their common G protein-signaling pathways is a more tractable alternative (17, 28, 29). This study focused on $G\alpha_{13}$, and our results imply a key role for GPCR signaling through $G\alpha_{13}$ in several distinct cell types and developmental processes.

The observation that *Tie2-Cre*-mediated excision of $G\alpha_{13}$ caused abnormal vascular structures and embryonic death beginning at E9.5 indicates a key role for $G\alpha_{13}$ in a *Tie2-Cre*-expressing lineage. *Tie2-Cre* can mediate excision of floxed alleles in both endothelium and in hematopoietic lineages (ref. 30 and data not shown). However, several observations point to an endothelial, rather than hematopoietic, defect as the cause of embryonic death in the *Tie2-*$Cre^{Tg/o}$; $G\alpha_{13}^{flox/-}$ embryos. Although the majority of endothelial cells in $G\alpha_{13}$ lacZ knockin embryos showed X-Gal staining at E9.5–10.5 (Fig. 1), <2% of circulating embryonic blood cells were lacZ-positive at this time (data not shown). Thus, $G\alpha_{13}$ may not normally be expressed in most embryonic blood cells. Similarly, X-Gal staining of E9.5 embryos bearing the *Tie2-*$G\alpha_{13}$ transgene, which rescued the early vascular development defect in $G\alpha_{13}^{-/-}$ embryos, revealed transgene expression in only a few percent of circulating blood cells. It is still formally possible that $G\alpha_{13}$ is important in hematopoietic stem cells that represent only a small fraction of circulating cells in the embryo. However, although defects in hematopoiesis can cause death of the embryo between E10.5 and 12.5, typically such affected embryos are morphologically indistinguishable from their WT littermates except for pallor (31–35). They do not exhibit the abnormal vascular structures, failed remodeling of blood vessels, and pericardial dilatation that were already present in $G\alpha_{13}$ endoKO embryos at E9.5). Thus, our

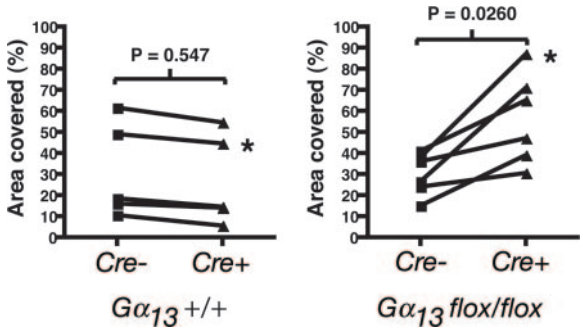

Fig. 6. $G\alpha_{13}$-deficient endothelial cells are impaired in their ability to form a network on Matrigel. $G\alpha_{13}^{flox/flox}$ or $G\alpha_{13}^{+/+}$ endothelial cells were infected with control GFP-adenovirus (Cre^-) or GFP-Cre adenovirus (Cre^+) then plated on Matrigel as described in *Supporting Methods*. The percent of the Matrigel surface covered with cells was calculated for five separate $G\alpha_{13}^{+/+}$ and six separate $G\alpha_{13}^{flox/flox}$ cell preparations. Connected points indicate paired samples from a single endothelial cell preparation infected with Cre^+ vs. Cre^- virus. Asterisks mark the samples shown in Fig. 7, which is published as supporting information on the PNAS web site. Note that network formation decreased (and, hence, area covered by cells increased) in association with Cre expression in $G\alpha_{13}^{flox/flox}$ but not WT endothelial cells. *P* values were calculated with the Mann–Whitney test.

Table 4. *Tie2-*$G\alpha_{13}$ transgene rescues development of endothelial conditional $G\alpha_{13}$ knockout mice

	flox/+	+/−	−/−	flox/−
Tie2-$G\alpha_{13}^{Tg/o}$	19	20	0	21
Tie2-$G\alpha_{13}^{o/o}$	25	18	0	0

Genotypes of 103 offspring from *Tie2-*$G\alpha_{13}^{Tg/o}$; $G\alpha_{13}^{flox/-} \times$ *Tie2-*$Cre^{Tg/Tg}$; $G\alpha_{13}^{+/-}$ intercrosses were determined at postnatal days 10–15. All carry the Tie2-Cre transgene such that all $G\alpha_{13}^{flox/-}$ are endothelial-specific knockouts. Note the complete rescue of the endothelial-specific knockouts by the transgene.

results are most consistent with the hypothesis that $G\alpha_{13}$ function in endothelial cells is necessary for proper vascular development.

The observation that the *Tie2-*$G\alpha_{13}$ transgene completely rescued development of $G\alpha_{13}$ endoKO embryos but not $G\alpha_{13}^{-/-}$ embryos suggests that $G\alpha_{13}$ function in cell types other than endothelial cells is important for embryonic development. Preliminary studies show that the exencephaly and intracranial hemorrhage exhibited by $G\alpha_{13}^{-/-}$ embryos bearing the endothelial transgene are phenocopied by *Wnt1-Cre*-mediated excision of $G\alpha_{13}$. This finding, coupled with our observation that $G\alpha_{13}$ is expressed in the dorsal neural tube at the time and place where neural crest cells delaminate, suggests that $G\alpha_{13}$ plays a role in the formation of neural crest or its derivatives (K. Ruppel and S. Coughlin, unpublished data).

Exactly how the loss of $G\alpha_{13}$ function in vascular endothelial interferes with vascular development is unknown. $G\alpha_{13}$ contributes to the regulation of the small GTPase Rho by GPCRs, and Rho plays a key role in regulation of the actin cytoskeleton and other cellular processes (36). We were unable to detect defects in GPCR-induced Rho activation, changes in cell shape, or chemokinesis of individual cells in $G\alpha_{13}$-null endothelial cells in culture. $G\alpha_{12}$ and $G\alpha_q$, both capable of regulating Rho, were expressed in these cultures (data not shown), and partial redundancy with these or other G proteins might mask effects of $G\alpha_{13}$ deficiency in these assays. A reproducible effect of $G\alpha_{13}$ deficiency was seen when endothelial cells were examined for a more complex behavior: the ability to form networks on Matrigel. Null cells tended to remain organized as sheets rather than reorienting to form networks of cords and tubes. Thus, $G\alpha_{13}$ likely helps orchestrate complex changes in cell shape, movement, and cell–cell and cell–matrix interactions required for vascular remodeling.

It is interesting to consider analogies between $G\alpha_{13}$ phenotypes and the concertina gastrulation defect. Concertina is the *Drosophila* homolog of $G\alpha_{13}$ (37). Gastrulation in fly embryos requires furrow formation and inward migration of cells at sites along the length of the embryo rather than through a single blastopore as in mouse. Concertina embryos begin a furrow by forming a zone of tightly apposed cells and do constrict the apices of some cells but not enough to form an organized groove (37). Thus, $G\alpha_{13}$ is not necessary for initiation of gastrulation in *Drosophila* but plays a necessary role in coordinating or propagating changes in cell shape and movement. This result may relate to the yolk sac vascular defects seen in our studies; endothelial cells form sheets and an initial plexus but fail to properly reorganize it. Detailed studies of the cytoskeletal rearrangements in WT and $G\alpha_{13}$-null endothelial cells and their movement during vertebrate vasculogenesis and angiogenesis are needed.

Studies of the signaling molecules that orchestrate the behavior of endothelial cells during blood vessel development have focused mainly on growth factors and receptor tyrosine kinases. Our results emphasize a role for GPCRs in this process. We previously showed that knockout of PAR1, a GPCR for thrombin, caused a partially penetrant embryonic lethality at midgestation that could be attributed to a role for PAR1 in endothelial cells (11, 14). This phenotype was similar in time of onset and general features to that observed in $G\alpha_{13}$ endoKO embryos in this study, but the latter phenotype was more severe and penetrant. Thus, the loss of $G\alpha_{13}$ activation by PAR1 in endothelial cells may account for the phenotype of $Par1^{-/-}$ embryos, but other endothelial GPCRs probably also contribute to $G\alpha_{13}$ activation in those cells. The observation that $G\alpha_{13}^{+/-}$ embryos showed virtually no embryonic lethality, $Par1^{-/-}$ embryos show ≈50% lethality, and $G\alpha_{13}^{+/-}$ $Par1^{-/-}$ embryos showed ≈100% lethality is consistent with this model (K.M.R. and S.R.C., unpublished data). Knockout of S1P1, a Gi-coupled receptor for sphingosine-1 phosphate (13), caused lethality that began at ≈E12.5 and was attributable to a necessary function in endothelial cells (15). Combined deficiency of this receptor with S1P2 and S1P3, which couple to Gi, Gq, and G12/13, yielded earlier phenotypes (16). Thus, multiple GPCRs play both unique and partially redundant roles in helping to orchestrate endothelial cell function during blood vessel development, and signaling through $G\alpha_{13}$ plays a key role in this process.

We thank Drs. Tom Sato and Mashashi Yanagisawa of the University of Texas Southwestern; J. Miyazaki of Osaka University Medical School; Marc Tessier-Lavigne of Genentech; Hilary Beggs, Louis Reichardt, and Gail Martin of the University of California, San Francisco; S.M. Dymecki, Carnegie Institute of Washington; Mel Simon of California Institute of Technology; and Andrew McMahon of Harvard University (Cambridge, MA) for specific plasmids and transgenic mouse lines (see *Materials and Methods*); and Pao-Tien Chuang, Didier Stainier, and Gail Martin for their critical reading of this manuscript. This work was supported in part by National Institutes of Health Grants HL65590 and HL44907 (to S.R.C.).

1. Risau, W. & Flamme, I. (1995) *Annu. Rev. Cell Dev. Biol.* **11,** 73–91.
2. Risau, W. (1997) *Nature* **386,** 671–674.
3. Carmeliet, P. (2000) *Nat. Med.* **6,** 389–395.
4. Sato, T. N., Tozawa, Y., Deutsch, U., Wolburg-Buchholz, K., Fujiwara, Y., Gendron-Maguire, M., Gridley, T., Wolburg, H., Risau, W. & Qin, Y. (1995) *Nature* **376,** 70–74.
5. George, E. L., Georges, L. E., Patel, K. R., Rayburn, H. & Hynes, R. O. (1993) *Development (Cambridge, U.K.)* **119,** 1079–1091.
6. Yang, J. T., Rayburn, H. & Hynes, R. O. (1993) *Development (Cambridge, U.K.)* **119,** 1093–1105.
7. Hellstrom, M., Kalen, M., Lindahl, P., Abramsson, A. & Betsholtz, C. (1999) *Development (Cambridge, U.K.)* **126,** 3047–3055.
8. Lindahl, P., Johansoon, B. R., Levéen, P. & Betsholtz, C. (1997) *Science* **277,** 242–245.
9. Levéen, P., Pekny, M., Gebre-Medhin, S., Swolin, B., Larsson, E. & Betsholtz, C. (1994) *Genes Dev.* **8,** 1875–1887.
10. Addison, C. L., Daniel, T. O., Burdick, M. D., Liu, H., Ehlert, J. E., Xue, Y. Y., Buechi, L., Walz, A., Richmond, A. & Strieter, R. M. (2000) *J. Immunol.* **165,** 5269–5277.
11. Connolly, A. J., Ishihara, H., Kahn, M. L., Farese, R. V., Jr., & Coughlin, S. R. (1996) *Nature* **381,** 516–519.
12. Yanagisawa, H., Hammer, R. E., Richardson, J. A., Williams, S. C., Clouthier, D. E. & Yanagisawa, M. (1998) *J. Clin. Invest.* **102,** 22–33.
13. Liu, Y., Wada, R., Yamashita, T., Mi, Y., Deng, C. X., Hobson, J. P., Rosenfeldt, H. M., Nava, V. E., Chae, S. S., Lee, M. J., *et al.* (2000) *J. Clin. Invest.* **106,** 951–961.
14. Griffin, C. T., Srinivasan, Y., Zheng, Y. W., Huang, W. & Coughlin, S. R. (2001) *Science* **293,** 1666–1670.
15. Allende, M. L., Yamashita, T. & Proia, R. L. (2003) *Blood* **102,** 3665–3667.
16. Kono, M., Mi, Y., Liu, Y., Sasaki, T., Allende, M. L., Wu, Y. P., Yamashita, T. & Proia, R. L. (2004) *J. Biol. Chem.* **279,** 29367–29373.
17. Offermanns, S., Mancino, V., Revel, J. P. & Simon, M. I. (1997) *Science* **275,** 533–536.
18. Sakai, K. & Miyazaki, J. (1997) *Biochem. Biophys. Res. Commun.* **237,** 318–324.
19. Plump, A. S., Erskine, L., Sabatier, C., Brose, K., Epstein, C. J., Goodman, C. S., Mason, C. A. & Tessier-Lavigne, M. (2002) *Neuron* **33,** 219–232.
20. Schlaeger, T. M., Bartunkova, S., Lawitts, J. A., Teichmann, G., Risau, W., Deutsch, U. & Sato, T. N. (1997) *Proc. Natl. Acad. Sci. USA* **94,** 3058–3063.
21. Kisanuki, Y. Y., Hammer, R. E., Miyazaki, J., Williams, S. C., Richardson, J. A. & Yanagisawa, M. (2001) *Dev. Biol.* **230,** 230–242.
22. Dymecki, S. M. (1996) *Gene* **171,** 197–201.
23. Soriano, P. (1999) *Nat. Genet.* **21,** 70–71.
24. Schlaeger, T. M., Qin, Y., Fujiwara, Y., Magram, J. & Sato, T. N. (1995) *Development (Cambridge, U.K.)* **121,** 1089–1098.
25. Kataoka, H., Hamilton, J. R., McKemy, D. D., Camerer, E., Zheng, Y. W., Cheng, A., Griffin, C. & Coughlin, S. R. (2003) *Blood* **102,** 3224–3231.
26. He, T. C., Zhou, S., da Costa, L. T., Yu, J., Kinzler, K. W. & Vogelstein, B. (1998) *Proc. Natl. Acad. Sci. USA* **95,** 2509–2514.
27. Beggs, H. E., Schahin-Reed, D., Zang, K., Goebbels, S., Nave, K. A., Gorski, J., Jones, K. R., Sretavan, D. & Reichardt, L. F. (2003) *Neuron* **40,** 501–514.
28. Offermanns, S. & Simon, M. I. (1998) *Oncogene* **17,** 1375–1381.
29. Offermanns, S., Zhao, L. P., Gohla, A., Sarosi, I., Simon, M. I. & Wilkie, T. M. (1998) *EMBO J.* **17,** 4304–4312.
30. Gitler, A. D., Kong, Y., Choi, J. K., Zhu, Y., Pear, W. S. & Epstein, J. A. (2004) *Pediatr. Res.* **55,** 581–584.
31. Tsai, F. Y., Keller, G., Kuo, F. C., Weiss, M., Chen, J., Rosenblatt, M., Alt, F. W. & Orkin, S. H. (1994) *Nature* **371,** 221–226.
32. Shimizu, R., Ohneda, K., Engel, J. D., Trainor, C. D. & Yamamoto, M. (2004) *Blood* **103,** 2560–2567.
33. Visvader, J. E., Fujiwara, Y. & Orkin, S. H. (1998) *Genes Dev.* **12,** 473–479.
34. Fujiwara, Y., Browne, C. P., Cunniff, K., Goff, S. C. & Orkin, S. H. (1996) *Proc. Natl. Acad. Sci. USA* **93,** 12355–12358.
35. Crispino, J. D., Lodish, M. B., Thurberg, B. L., Litovsky, S. H., Collins, T., Molkentin, J. D. & Orkin, S. H. (2001) *Genes Dev.* **15,** 839–844.
36. Hall, A. (1998) *Science* **279,** 509–514.
37. Parks, S. & Wieschaus, E. (1991) *Cell* **64,** 447–458.